Journal of Nano- and Electronic Physics
Vol. **14** No 2, 02007(5pp) (2022)

Журнал нано- та електронної фізики
Том **14** № 2, 02007(5cc) (2022)

Effect of the Conduction Band Offset on the Performance of GaAs/$Al_xGa_{1-x}As$ Resonant Tunneling Diode

M. Charmi*

Department of Nano Physics, Malekashtar University of Technology, Shahinshahr, Isfahan, Iran

(Received 05 February 2022; revised manuscript received 16 April 2022; published online 29 April 2022)

This paper presents the effects of conduction band offset and aluminum mole fraction on performance of GaAs/$Al_xGa_{1-x}As$ resonant tunneling diode using full quantum simulation. The simulation is based on a self-consistent solution of the Poisson equation and Schrodinger equation with open boundary conditions, within the non-equilibrium Green function formalism. A resonant tunneling diode structure consists of a 2 nm narrow band gap, a quantum well of GaAs is sandwiched between two thin wide band gap barriers of AlGaAs with a width of 2 nm. These three layers are sandwiched between two un-doped GaAs spacer layers with a width of 15 nm that are connected to two large reservoirs of high dopant GaAs contacts (10^{18} cm^{-3}) with a width of 12 nm. The effects of varying Al mole fraction are investigated in terms of the conduction band, transmission function and output current. Simulation results illustrate that the device performance can be improved by proper selection of the mole fraction.

Keywords: Conduction band offset, Non-equilibrium Green function (NEGF), Resonant Tunneling Diode (RTD), Al mole fraction, Quantum transport.

DOI: 10.21272/jnep.14(2).02007 PACS numbers 73.23.Ad, 73.61.Ey, 73.40.Gk

1. INTRODUCTION

Double barrier quantum well resonant tunneling diodes (DBQW RTDs) are based on quantum tunneling mechanisms, with the carrier transport being perpendicular to the DBQW plane. RTDs are excellent candidates for nanoelectronic circuit applications due to their wide-band width negative differential conductance (NDC), pronounced nonlinear current-voltage characteristic, inherent high speed, structural simplicity, relative ease of fabrication, flexible design, and versatile circuit functionality [1, 2]. Very high-speed operation arises from the extremely small size of the RTD structure along the direction of carrier transport and the tunneling process responsible for carrier flow [3, 4]. RTDs present very attractive characteristics, such as a high intrinsic cut-off frequency (theoretical value in the THz range) and current peaks associated with negative differential resistance (NDR) regions. These RTD specificities are exploited in digital applications such as memory applications [5] and analog to digital converter [6, 7] as well as analog applications such as frequency divider [8], frequency multiplier [9], and oscillator [10], leading to simpler circuits reducing the circuit size with a large gain in power consumption and high frequency performance.

Small electron effective mass and low band offset in III-V heterostructures make these materials interesting candidates for RTD fabrication [11]. Among the III-V based RTDs, GaAs/AlGaAs systems remain one of the best options due to the experience gained on the fabrication of this technology, and the Al mole fraction (x parameter) in the $Al_xGa_{1-x}As$ structure is important parameter that varies the band structure. In this work, the impact of conduction band offset and mole fraction of Al in GaAs/AlGaAs RTD has been investigated. The simulations have been done by self-consistently solving the Poisson equation and the Schrodinger equation with open boundary conditions, within the non-equilibrium Green function (NEGF) formalism.

2. DEVICE STRUCTURE AND SIMULATION APPROACH

RTD is a two terminal electronic device that consists of a narrow band gap layer (quantum well) sandwiched between two thin wide band gap layers (barriers). A schematic layer structure of the RTD employed in this project is shown in Fig 1. It is noted that un-doped gallium arsenide (GaAs) is sandwiched between two thin un-doped aluminum gallium arsenide (AlGaAs) layers. Because of the difference of these two semiconductor material band gaps, a double barrier quantum well (DBQW) is formed. An un-doped GaAs quantum well with a width of 2 nm, two un-doped AlGaAs barriers with a width of 2 nm, two un-doped GaAs spacer layers with a width of 15 nm nearby the barrier and two high dopant GaAs contacts (10^{18} cm) with a width of 12 nm that are connect to the two large reservoirs. To increase the current density through the device, heavily doped contacts are used which can supply a large number of electrons. High doping gives rise to high levels of impurity scattering which can destroy the wave coherence of electrons in the well that is necessary for resonant transmission. Therefore, low doped or un-doped spacer layers are used in between the un-doped barrier/well/barrier region and the doped contacts to prevent diffusion of impurity atoms into the barriers and well.

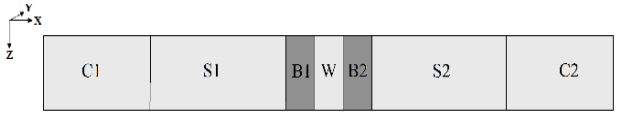

Fig. 1 – Schematic cross-sectional view of RTD

* charmi.phy@gmail.com

Since transport happens in one direction, within effective mass formulism, the device could be represented by a one-dimensional chain of nodes with spatially varying effective mass at material interface and periodic boundary condition to other two directions (Fig. 1). In the transport direction (the x-direction), the NEGF approach, which is equivalent to solving the Schrödinger equation with open boundary conditions, is used to describe the ballistic quantum transport. The retarded Green function for the device in matrix form is computed as [12-14]:

$$G(E)=\left[(E+i\eta)I-H-\Sigma_1-\Sigma_2\right]^{-1}, \quad (1)$$

where Σ_1 and Σ_2 are the self-energies of the emitter and collector contacts, respectively, which represent the effects on the finite device Hamiltonian due to the interactions of the channel with the emitter/collector contacts, η is an infinitesimal positive value, E is the energy, I is the identity matrix, and H is the Hamiltonian of the resonant tunneling diode. As can be seen from Eq. (1), the transport is assumed here to be completely ballistic. The spectral density functions due to the contacts can be obtained as:

$$A_1=G\Gamma_1G^{\dagger} \quad \text{and} \quad A_2=G\Gamma_2G^{\dagger}, \quad (2)$$

where $\Gamma_1=i\left(\Sigma_1-\Sigma_1^{\dagger}\right)$ and $\Gamma_2=i\left(\Sigma_2-\Sigma_2^{\dagger}\right)$. The source related spectral function is filled up according to the Fermi energy in the source contact, while the drain related spectral function is filled up according to the Fermi energy in the drain contact, and diagonal entries of spectral functions represent local density-of-states at each node [12]. From equation (1) and (2), we can obtain the 2D electron density matrix. The electron density is fed back to the Poisson equation solver for the self-consistent solution. Once self-consistency is achieved, the terminal current can be expressed as a function of the transmission coefficient. The transmission coefficient from contact1 to contact2 is defined in terms of the Green function as [12]:

$$T(E)=\text{trace}\left(\Gamma_1(E)G(E)\Gamma_2(E)G^{\dagger}(E)\right). \quad (3)$$

It is straightforward to write the emitter-collector current as:

$$I_{1-2}=\left(\frac{-q}{h}\right)\int_{-\infty}^{+\infty}dE\cdot T(E)\cdot(F_0(E-\mu_1)-F_0(E-\mu_2)), \quad (4)$$

where q is the electron charge, h is the Plank constant, F_0 is the Fermi-Dirac integral of order 0 [15, 16], μ_1 is the Fermi level of contact1 and μ_2 is the Fermi level of contact2.

3. RESULTS AND DISCUSSION

The properties of III-V compound semiconductors and their heterojunctions have been relentlessly investigated for several decades due to their wide-ranging applications in electronic and optoelectronic technologies. One of the most important electronic properties of heterojunctions is the band offset, which describes the relative alignment of the electronic bands across the junction interface. An accurate determination of the band offset is critical for understanding quantum transport properties of heterojunctons. For many III-V materials systems, the band offset has been carefully measured experimentally and theoretically [17-20]. The energies of the conduction band minima in AlGaAs relative to the top of the valance band at the Γ point (in electron volts at 300 K), as a function of Al mole fraction, are given by

$$E_g^{\Gamma}=1.424+1.247x,\ x\le 0.45, \quad (5)$$

$$E_g^{\Gamma}=1.424+1.247x+1.147\left(x-0.45\right)^2, x>0.45, \quad (6)$$

$$E_g^{L}=1.708+0.642x, \quad (7)$$

$$E_g^{X}=1.900+0.125x+0.143x^2. \quad (8)$$

These equations are plotted in Fig. 2. As the Al mole fraction in $Al_xGa_{1-x}As$ is increased from 0 to 1, the band gap of the resulting alloy increases from that of GaAs to that of AlAs. For Al mole fraction $x \le 0.45$, the Γ-valley provides the conduction band minimum, while for $x > 0.45$ the X-valley is the lowest conduction band minimum. The L-valley has an energy intermediate between the Γ and X-valley and plays no part in the discussion. For aluminum mole fraction less than 0.45, the conduction band discontinuity is:

$$\Delta E_c=0.81x,\ x\le 0.45. \quad (9)$$

The conduction band offset has been experimentally obtained by several groups on heterojunctions [21-23]. For aluminum mole fraction greater than 0.45, AlGaAs has an indirect band gap with the X-valley lowest in energy. The band gap in this region increases slowly with increasing mole fraction in comparison to the rapid increase in the Γ-valley energy (Fig. 2). The conduction band discontinuity for mole fraction greater than 0.45 is given by:

$$\Delta E_c=0.395+0.05x-0.143x^2, x>0.45. \quad (10)$$

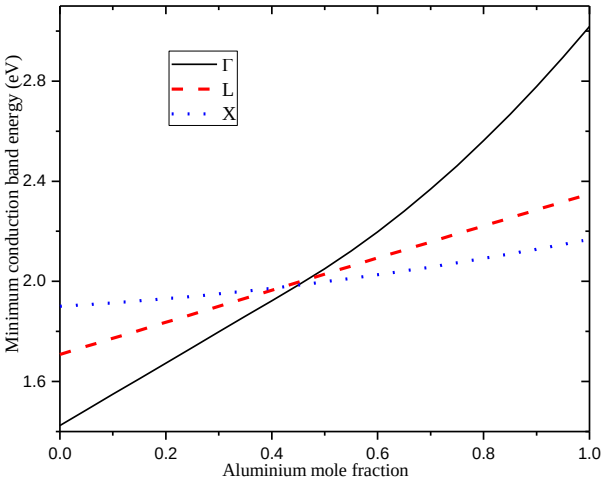

Fig. 2 – Minimum conduction band energy versus Al mole fraction for Γ, X and L valleys of GaAs/AlGaAs heterojunction

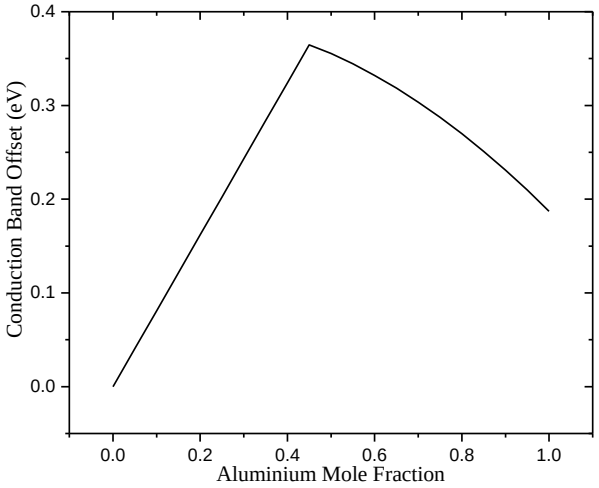

Fig. 3 – Conduction band discontinuity for direct (Γ) and indirect (X) gaps versus Al mole fraction of RTD

Equations (9) and (10) are plotted in Fig. 3. It is clear that for $x \leq 0.45$, with increasing x, the conduction band offset is linearly increased and reaches 0.36 eV. For $x > 0.45$, with increasing Al mole fraction, the conduction band offset is decreased and achieves 0.19 eV. The maximum conduction band discontinuity is approximately 0.36 eV and occurs for Al mole fraction of 0.45, corresponding to the transition from direct to indirect AlGaAs. This is important for optimizing heterojunction GaAs devices such as HBJTs, HEMTs and RTDs. In RTDs, due to a decrease in the conduction band offset for a mole fraction greater than 0.45, the properties of RTDs are investigated by consideration of only Al mole fraction between 0-0.45. The magnitude of the band offset creating the quantum well should be large enough to obtain a confined quantum well state.

The conduction band profile under non-equilibrium conditions is obtained by adding the self-consistent potential energy to the equilibrium conduction band profile. Fig. 4 shows the conductions band profile at 0.6 V versus different Al mole fractions obtained from quantum self-consistent calculation. The Al mole fraction has a value of $x = 0.1$, 0.23, 0.3, 0.4 and 0.45. The barrier height is an important parameter in RTDs that has ability to effect change in the peak current density, transmission coefficient and PVCR (peek to valley current ratio). With increasing x, the height of the barrier (height of AlGaAs) is increased that leads to a deep potential well. So, for each mole fraction we have different barrier heights and different peak currents and PVCR. Therefore, the mole fraction in RTDs is the most parameter that must be considered, and the trade-off between large peak current density and large PVCR is achieved by adopting different mole fractions.

Fig. 5 shows the transmission function for RTD at 0.6 V bias. Each peak of the transmission function corresponds to the resonance energy in the quantum well. It is shown that for Al mole fraction of 0.1, the transmission is identical for all energies and there is no peek also for Al mole fraction less than 0.23. This means that, due to the low barrier height, all electrons can pass over the barrier, and RTD appears to be completely transparent at all energies of the incident electron. With increasing mole fraction from 0.23 to 0.45,

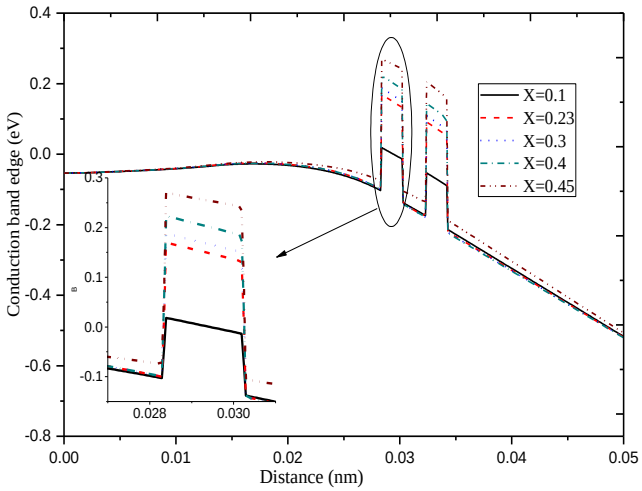

Fig. 4 – Conduction band edge for Al mole fraction of less than 0.45

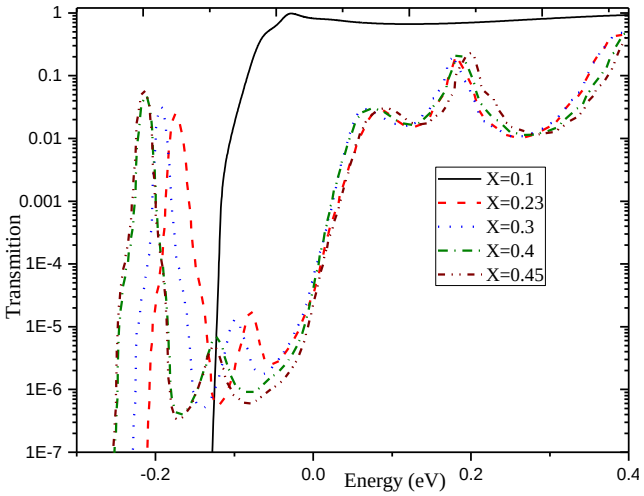

Fig. 5 – Transmission function for different Al mole fractions

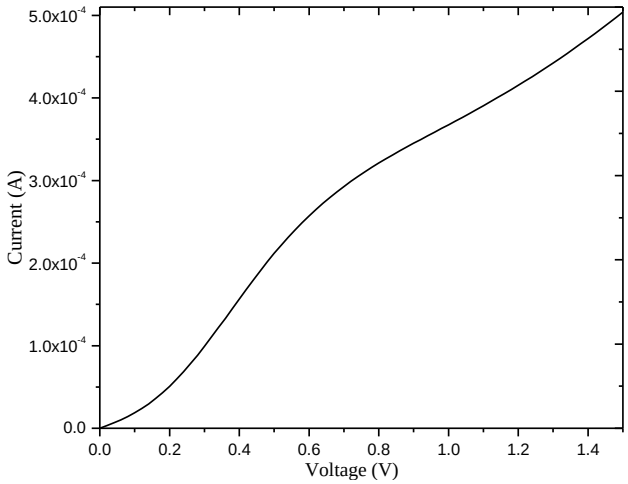

Fig. 6 – Output current versus input voltage only for Al mole fraction of 0.1

the barrier height increases and electron tunneling through the barriers is strongly enhanced, when its energy equals to one of the energy levels in the quantum well, the maximum transmission probability is possible. This corresponds to resonant tunneling, and

the DBQW structure acts as a filter, so that only electrons with energies close to the resonance energies have a high probability of crossing the two barriers.

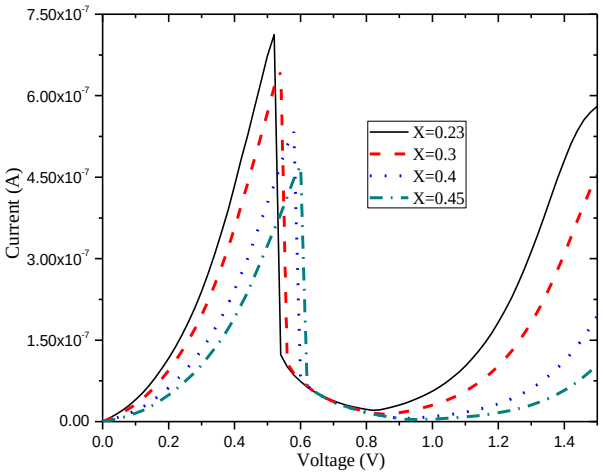

Fig. 7 – Output current versus input voltage for different Al mole fractions

The output current of RTD for a mole fraction of 0.1 is plotted in Fig. 6. Due to low barrier height the electron can pass over the barrier, there is no NDR for a mole fraction less than 0.23. While for a mole fraction from 0.23 to 0.45, the tunneling current at resonant energy was observed. It is clear from Fig. 7 and Table 1 that, with increasing Al mole fraction, the peak current (I_P) decreases, the valley current (I_V) decreases, the peak-to-valley current ratio (PVCR) increases and the voltage at the peak current (V_P) increases. In a deeper quantum well (higher mole fraction), the resonance energy level will push up, thus the resonant tunneling will occur at high bias voltage, resulting in a shift of the peak voltage V_P to the right and a decrease in the peek current I_V. The valley current arising from the off resonance is decreased by increasing the mole fraction that leads to an increase in PVCR. A high peak current is required for high-speed applications and for many analog applications that is achieved with low mole fraction ($x = 0.23$). PVCR is an important figure of merit of RTD for both analog and digital applications that is achieved with high mole fraction ($x = 0.45$). The high barrier height reduces the peak current density but provides high transmission coefficient benefiting large PVCR. In practice, the trade-off between large peak current density and large PVCR is achieved by adopting different Al mole fraction (for example at $x = 0.4$).

Table 1 – *I-V* characterizations of RTD for different Al mole fractions

Al mole fraction	I_P (A)	I_V (A)	PVCR	V_P (V)
0.23	7.12×10^{-7}	2.09×10^{-8}	34.1	5.2
0.3	6.51×10^{-7}	1.34×10^{-8}	48.4	5.4
0.4	5.34×10^{-7}	5.76×10^{-9}	92.8	5.8
0.45	4.71×10^{-7}	3.44×10^{-9}	136.7	0.6

4. CONCLUSIONS

The novel design considerations of Al mole fraction in GaAs/$Al_xGa_{1-x}As$ RTD are studied using quantum simulation within the NEGF formalism. The effects of the mole fraction parameter on device performance are carried out in terms of the conduction band, transmission function and output current. The results show that for the nominal mentioned RTD, there is no NDR for a mole fraction less than 0.23, and the trade-off between large peak current density and large PVCR is achieved by adopting different Al mole fractions that the optimum value is $x = 0.4$.

REFERENCES

1. J.P. Sun, G.I. Haddad, P. Mazumder, J.N. Schulman, *Proc. IEEE* **4**, 641 (1998).
2. P. Mazumder, S. Kulkarni, M. Bhattacharya, J.P. Sun, G.I. Haddad, *Proc. IEEE* **4**, 664 (1998).
3. H. Eisele, *Electron. Lett.* **46**, 8 (2010).
4. C. O'Sullivan, J. Murphy, *Field Guide to Terahertz Sources, Detectors, and Optics* (SPIE Press: 2012).
5. S.J. Wei, H.C. Lin, *IEEE J. Solid-State Circuit.* **27**, 212 (1992).
6. S.J. Wei, H.C. Lin, R.C. Potter, D. Shupe, *IEEE J. Solid-State Circuit.* **28**, 697 (1993).
7. T.P.E. Broekaert, B. Brar, J.P.A. van der Wagt, A.C. Seabaugh, T.S. Moise, F.J. Morris, E.A. Beam III, G.A. Frazier, *IEEE J. Solid-State Circuit.* **33**, 1342 (1998).
8. Y. Kawano, Y. Ohno, S. Kishimoto, K. Maezawa, T. Mizutani, *Electron. Lett.* **38**, 305 (2002).
9. U. Auer, W. Prost, G. Janßen, M. Agethen, R. Reuter, F.J. Tegude, *IEEE J. Select. Topic. Quantum Electron.* **2**, 650 (1996).
10. V.M. Bao, et al., *IEEE J. Solid-State Circuits* **39**, 1352 (2004).
11. T.J. Shewchuk, P.C. Chapin, P.D. Coleman, W. Kopp, R. Fischer, H. Morkoç, *Appl. Phys. Lett.* **46**, 508 (1985).
12. S. Datta, *Superlattice. Microst.* **28**, 253 (2000).
13. S. Datta, *Quantum Transport: Atom to Transistor* (Cambridge Univ. Press: Cambridge: 2005).
14. S. Datta, *Lessons from Nanoscience: A Lecture Note Series* (World Scientific Publishing Co. Pte. Ltd.: 2012).
15. M. Goano, *Solid-State Electron.* **36**, 217 (1993).
16. P.V. Halen, D.L. Pulfrey, *J. Appl. Phys.* **57**, 5271 (1985).
17. A. Franciosi, C.G. Van de Walle, *Surf. Sci. Rep.* **25**, 1 (1996).
18. I. Vurgaftman, J.R. Meyer, L.R. Ram-Mohan, *J. Appl. Phys.* **89**, 5815 (2001).
19. I. Vurgaftman, J.R. Meyer, L.R. Ram-Mohan, *Heterostructure Laser, Part A: Fundamental Principle* (Academic Press: New York: 1978).
20. J. Batey, S.L. Wright, D.J. Dimaria, *J. Appl. Phys.* **57**, 484 (1985).
21. Y. Wang, F. Zahid, Y. Zhu, L. Liu, J. Wang, H. Guo, *Appl. Phys. Lett* **102**, 132109 (2013).
22. W.L. Wang, F. Stern, *J. Vac. Sci. Technol. B* **3**, 1280 (1985).
23. A.J. Hill, P.H. Ladbrooke, *Electron. Lett.* **22**, 218 (1986).

Вплив зсуву зони провідності на характеристики резонансного тунельного діода GaAs/Al$_x$Ga$_{1-x}$As

M. Charmi

Department of Nano Physics, Malekashtar University of Technology, Shahinshahr, Isfahan, Iran

У роботі представлено дослідження впливу зсуву зони провідності та молярної частки алюмінію на характеристики резонансного тунельного діода GaAs/Al$_x$Ga$_{1-x}$As з використанням повного квантового моделювання. Моделювання базується на самоузгодженому розв'язанні рівняння Пуассона та рівняння Шредінгера з відкритими граничними умовами в рамках формалізму нерівноважної функції Гріна. Структура резонансного тунельного діода складається з вузької забороненої зони 2 нм, квантова яма GaAs затиснута між двома тонкими широкозонними бар'єрами з AlGaAs шириною 2 нм. Ці три шари затиснуті між двома нелегованими роздільними шарами з GaAs шириною 15 нм, які з'єднані з двома великими резервуарами контактів GaAs з високим вмістом легуючих домішок (10^{18} см$^{-3}$) завширшки 12 нм. Досліджено вплив змінної молярної частки Al на зону провідності, функцію пропускання та вихідним струм. Результати моделювання показують, що характеристики пристрою можуть бути покращені шляхом правильного вибору молярної частки.

Ключові слова: Зсув зони провідності, Нерівноважна функція Гріна, Резонансний тунельний діод, Молярна частка Al, Квантовий транспорт.